Optica Applicata, Vol. XLIX, No. 2, 2019
DOI: 10.5277/oa190215

On the possibility of using arc plasma melting technique in preparation of transparent yttria ceramics

ANDRZEJ KRUK[1*], BENEDYKT R. JANY[2], KAROLINA OWCZARCZYK[3], DOMINIKA MADEJ[4]

[1]Pedagogical University of Cracow, Institute of Technology, Kraków, Poland

[2]Marian Smoluchowski Institute of Physics, Jagiellonian University, Lojasiewicza 11, 30-348 Kraków, Poland

[3]Centre for Nanometer-Scale Science and Advanced Materials, NANOSAM, Faculty of Physics, Astronomy and Applied Computer Science, Jagiellonian University, Lojasiewicza 11, 30-348 Kraków, Poland

[4]AGH University of Science and Technology, Faculty of Materials Science and Ceramics, Department of Ceramics and Refractories, Mickiewicza 30, 30-059 Kraków, Poland

[*]Corresponding author: andrzej.kruk@up.krakow.pl

A state-of-the-art fabrication of Y_2O_3 transparent ceramic by arc plasma synthesis using commercial micron-size powders is reported. The morphological observations of the surface by scanning electron microscope shows that a dense microstructure can be obtained. Arc melted samples are made of a white core and transparent layer. X-ray diffraction studies and also Raman spectroscopy confirm that only one phase occurred in the core and in the transparent layer, and that the physicochemical difference exists. The obtained Y_2O_3 shell ceramics have pores but also relative low absorbance in the VIS-NIR region after double side polishing. The optical band gap and the refractive index are reported. It is concluded that arc plasma melting allows obtaining quickly (10 minutes) dense and highly transparent polycrystalline samples, especially in the VIS-IR spectral region.

Keywords: plasma arc melting, transparent ceramic, yttrium oxide, optical properties.

1. Introduction

Polycrystalline yttrium oxide has been widely investigated as a potential material for laser technology, semiconductor technology, heavy industry and many others applications [1–10]. Yttria is characterized by a series of positive physicochemical properties, such as a broad transparency range (*ca*. 0.3–8 μm), where theoretical transmittance is over 80% for visible light and 65% for infrared light, as well as strong absorbance in ultraviolet light, refractive index (*ca.* 2.2), high thermal conductivity (13.6 W/m·K),

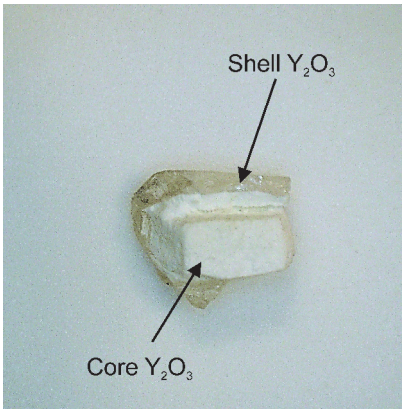

Fig. 1. Photography of cross-section Y_2O_3 obtained after PAM.

very good chemical stability and also by a low thermal expansion coefficient [1–10]. Additionally, it is possible to incorporate metal and rare earth elements into the yttrium oxide lattice, low energy cut-off of phonons (591 cm^{-1}) [8–10] and energy gap (approximately 4–5.5 eV) [3–6]. According to Mie's scattering theory [11], high optical transmittance of polycrystalline ceramic can be achieved by fabricating pore-free and high purity ceramic. Four popular methods: vacuum sintering, spark plasma sintering, hot pressing and hot isostating pressing [3, 6, 7, 11–28] are widely used to obtain a dense and translucent oxide ceramic. In contrast to these methods, an arc plasma melting technique requires high purity powders only, without any other requirements, because of size, the shape and distribution of particles and agglomerates have no influence on the pores creation during the melting process.

The Y_2O_3 polycrystalline ceramics are very extensively investigated from the point of view of physicochemical properties. In this paper, an alternative technique plasma arc melting (PAM) was used. After PAM a sample is built with a white not fully-melted core and full-melted the transparent shell (Fig. 1). A detailed study of the physicochemical properties focused on a difference between the core and the shell of arc plasma melted Y_2O_3. In this paper, the optical properties of the shell plasma arc melted Y_2O_3 transparent ceramics in UV-NIR spectrum were examined and presented in this study.

2. Experiment

2.1. Sample preparation

Commercial Y_2O_3 powder (Sigma-Aldrich, 99.99% purity) with a mean particle diameter of 2.0 μm was chosen as material. The powder was ground in an agate mortar and sieved through a 50-mesh screen, finally pressed at 20 MPa into ∅23 mm pellets in a zirconium mould. In the arc furnace, equipped with a tungsten electrode and connected with a high efficiently water cooled copper crucible, arc plasma synthesis was conducted. The melting of Y_2O_3 green bodies was conducted in an inert gas environ-

ment of an argon flow (99% purity). Finally, the material was cooled down at an approximate cooling rate of 19 K/s in the first seconds. A polycrystalline Y_2O_3 bulk sample in transparent layer (shell) and a white core was obtained. Finally, parts of the samples were mechanical separated and the transparent shell was double-side polished. A representative sample from the arc melted ceramics was selected.

2.2. Methodology

The Panalytical X'Pert was used for X-ray diffraction (XRD) measurements with CuK_α radiation. The diffraction pattern was measured with 2θ range 17°–80°, and a step of 0.08°, counting time of 30 s/step. The qualitative phase analysis was performed with the use of Highscore Plus software (Panalytical) and a standard data set of PCPDFWIN version 2.3. All parameters in the constituent phases were determined on the basis of the Rietveld profile refinement method.

The micromorphology of samples was observed with a scanning electron microscope (SEM) FEI Quanta 3D FEG with an energy-dispersive X-ray (EDAX SDD Apollo XP) used to examine chemical composition of the sample.

Free software ImageJ version 1.50i was used to obtain an area of pore distribution after processing a series of SEM microphotographs.

Horiba LabRam HR800 spectrometric analyzer was used to obtain Raman spectra in the range of 300–3500 cm^{-1}, with 1.5 cm^{-1} step, laser light source at 532 nm.

The absorption of Y_2O_3 was performed using the Specord 210 V Plus Analytik Jena. The shell thickness was *ca.* 1 mm after double side polishing.

3. Results and discussion

Figure 2 shows the XRD patterns recorded for the core and transparent layer Y_2O_3 obtained after PAM. The XRD patterns of Y_2O_3 are indexed as the cubic of Y_2O_3 (JCPDS

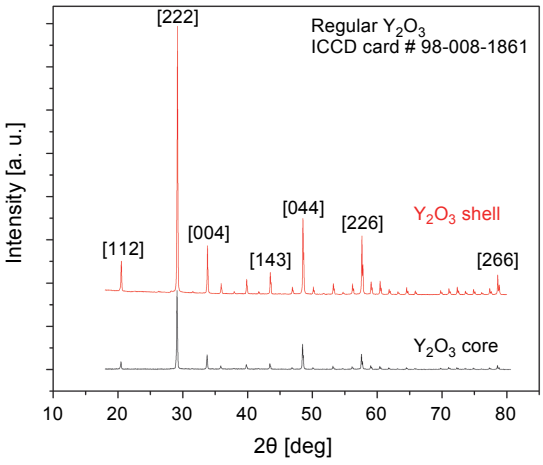

Fig. 2. XRD patterns of the core and the shell Y_2O_3 obtained after PAM.

T a b l e 1. Lattice spacing d_{hkl}, lattice parameter a and unit cell volume V with the crystallite size D_{XRD} and dislocation density ρ of PAM Y_2O_3.

	Shell	Core
d_{hkl} [nm]	3.0518	3.0662
a [Å]	10.5718	10.6216
V [Å^3]	1181.517	1198.3214
D_{XRD} [nm]	95.05	69.05
ρ [10^{-5} m^{-2}]	11.1	21

card # 98-008-1861) with the Ia-3 space group. The XRD pattern of the core and shell, reveals sharp well-defined peaks of pure yttria of regular structure without any detectable secondary phases. The approximated value of the lattice spacing d_{hkl}, the lattice parameter and unit cell volume V with the calculated crystallite size D_{XRD} and also dislocation density ρ of the investigated core and shell melted Y_2O_3 are presented in Table 1. The lattice parameter of core Y_2O_3 is very close to the theoretical value of pure Y_2O_3 of 10.604 Å. The difference between the experimental values results from the measurement error (*ca*. 3%) and the possible impurities. To estimate the minimum dislocation density of the particular structure, we use the following relation [27]:

$$\rho \approx \frac{1}{\langle D_{XRD} \rangle^2} \tag{1}$$

The dislocation density of the core and shell are calculated to be ~21 × 10^{-5} and 11.1 × 10^{-5} m^{-2}, respectively.

Figure 3**a** shows the microphotograph of the polished and thermally etched (1000°C, 1 hrs, flow Ar) surface of PAM Y_2O_3 sample [29]. The surface shows a fine micro-

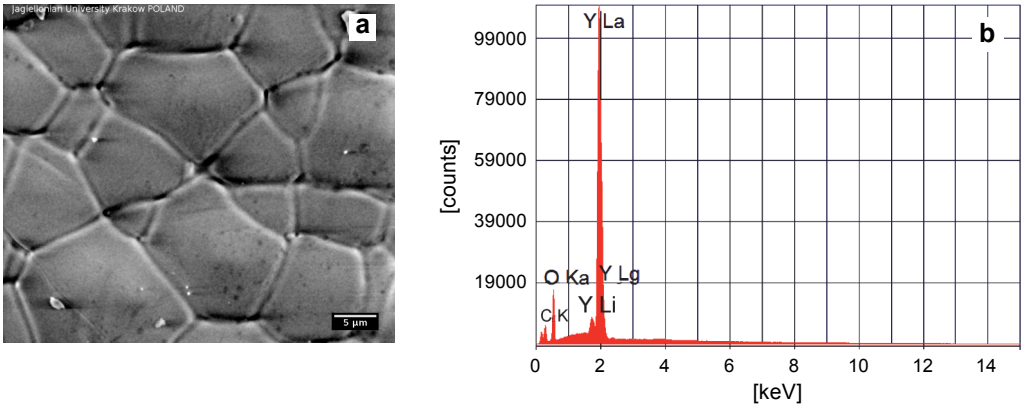

Fig. 3. SEM microphotograph of the polished and thermally etched surface of arc plasma melted Y_2O_3 sample after 1 hrs etching in argon (**a**), and results of the EDS surface analysis (**b**).

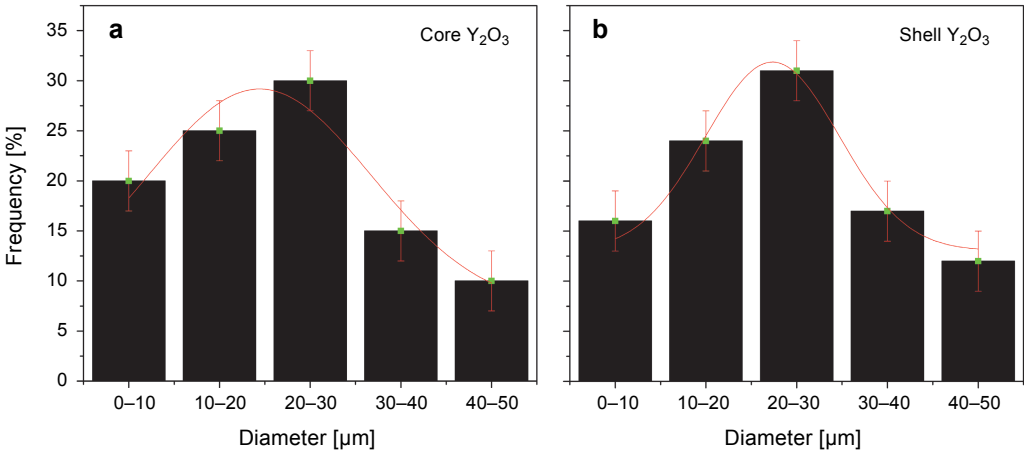

Fig. 4. Distribution of maximum grain diameters of the core (**a**) and shell (**b**) PAM-Y_2O_3.

structure with well-developed, irregular grains of *ca.* 5–30 μm. The grain boundaries are sharply defined and the major radius of grain ranged between 1 and 50 μm for the core and the shell PAM Y_2O_3. For the shell, the diameters of grains were mostly in a range from 20 to 30 μm, with a smaller number of small grains (above 10 μm). In the case of fully melted Y_2O_3, the average diameter of grains is higher than for core Y_2O_3. The results of EDS chemical composition analysis performed for the sample are presented in Fig 3**b**. The chemical composition corresponded to the composition of the Y_2O_3. The distribution of maximum grain diameters is one modal for two exanimate samples as shown in the histogram in Fig. 4. The smaller grains exhibit more frequency in the core Y_2O_3. The distribution of maximum diameters can be described with a Gauss function with good approximation. A small amount of isolated pores with a diameter that does not exceed 1 μm is located in the grain boundary. No pores are observed inside the grains in both samples. The mean area of pores is *ca.* 0.25 μm^2 and most pores are above 100 nm^2. Porosity is one of the major reasons for relatively low transparence, according to Mie's theory [11]. In order to improve the optical transmittance of the yttria ceramics, the plasma arc melting process and controlled speed cooling were involved to overcome the porous microstructure and cracking problems. The results of a standard quantitative EDS analysis of shell Y_2O_3 confirm the chemical element composition (Table 2). Carbon comes from a thin layer deposited prior to the SEM imaging.

T a b l e 2. EDX chemical elements content of Y_2O_3.

Chemical element	Core		Shell	
	At [%]	Net intensity	At [%]	Net intensity
O	53.19	700.56	55.31	720.87
Y	29.54	6804.56	28.35	7009.16

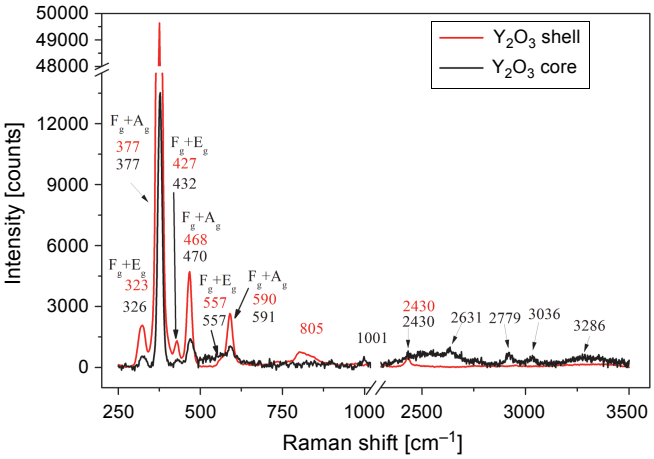

Fig. 5. Raman spectra of plasma arc melted Y_2O_3.

Figure 5 shows the Raman measurements of the shell and the core Y_2O_3 sample are in good agreement with what was observed in [31, 32]. All peaks around 250–700 cm^{-1} correspond to the vibration and oscillation type of the Y–O bonds. The most intense group of bands in all Raman spectra is observed in a 320 to 600 cm^{-1} range indicating a large polarizability variation. The peaks for layer subsequently decreased *ca.* 1–5 cm^{-1}. The reason is a decrease of grain size which is consistent with XRD results. In a wide range of Raman spectra between 1000 and 2400 cm^{-1} no peaks were detected. Raman spectra confirm the presence of only one cubic phase in both samples, like XRD results.

Spectrophotometric measurements for the layer Y_2O_3 were performed in the UV-VIS-NIR range (200–1100 nm), with a step of 1 nm (Fig. 6). The core is white in color and absolutely not translucent in the whole spectrum region. In the UV region, shells have no transmittance and the absorbance strongly decreased with increased

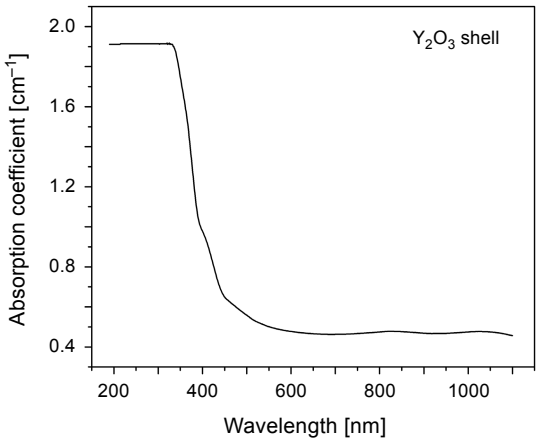

Fig. 6. UV-IR absorbance spectra of Y_2O_3 shell after plasma arc synthesis.

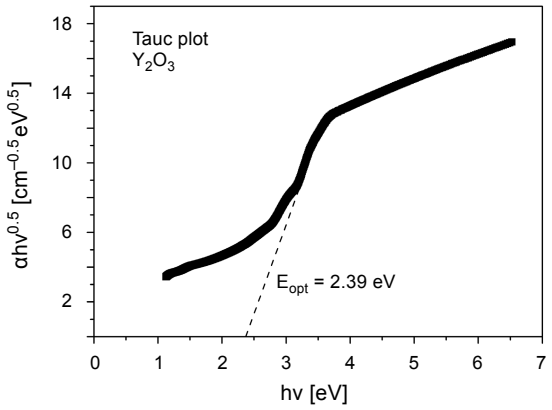

Fig. 7. Tauc plot (optical band gap) of Y_2O_3 shell after plasma arc synthesis.

wavelength. The highest transmittance of the sample is close to 50% from the VIS to NIR light especially in the 600–1100 nm wavelength range. No absorption centers were found. Those spectrophotometric features make Y_2O_3 suitable for use as a window in high temperature furnaces and for other optics applications. For certain levels of sinter transparency it is important to choose the slower cooling conditions for the melting process in order to reduce the number of pores.

Figure 7 displays a plot according to the Tauc relationship [32]. The empirical formula allows to estimate the energy of the gap E_g, by relating optical absorption coefficient α and the photon energy $h\nu$:

$$C(h\nu - E_g) = (h\nu)^t \tag{2}$$

where h is Planck constant (eV · s) and ν is frequency of the light (Hz), t is index having values of 1/2, 3/2, 2 and 3, depending on the type of electronic transition (direct, indirect, allowed, forbidden, respectively), C is an energy-independent value.

Extrapolation of the linear part of the graphs (Fig. 7) leads to an optical band gap E_{opt} width of 2.39 eV for arc melted Y_2O_3 in the case of direct transition (Eq. (3)). The optical and electronic band gaps are essentially identical, and the distinction between them is ignored. The presence of two or more slopes suggests that the samples have some impurities [34]. The determined energy band is consistent with other papers [3–6] and confirms a semiconductor behavior. The absorption coefficient was accurately calculated using the Beer–Lambert–Bouguer law. To calculate absorption coefficient the refractive index value 2.2–1.89 dependent on the wavelength was used [33].

Finally, a refractive index n was determined, using the equation proposed by DIMITROV [34], taking E_{opt} = 2.39 eV:

$$\frac{n^2 - 1}{n^2 + 1} = 1 - \sqrt{\frac{E_{opt}}{20}} \tag{3}$$

The refractive index n was calculated as 2.19 for fully melted Y_2O_3 in the VIS region. According to NIGARA [34], the value of parameter n in 0.36–1.2 μm spectral range changes between 2.2–1.89. Thus the refractive index n calculated with that method agrees with the values found in [33].

4. Conclusions

The Y_2O_3 transparent ceramic was fabricated successfully with an alternative technique of plasma arc melting. The homogenous microstructure of melted Y_2O_3 consists of grains with the average size of about 10 μm with small amount of nano-sized pores. The XRD study and Raman spectroscopy confirm only the cubic structure in both layers. Shifts in the rotational-vibrational spectra of both the shell and the core of arc-melted Y_2O_3 were shown and discussed. The optical band gap and the refractive index were calculated. Conditions of conducting arc plasma melting process should be improved. A PAM technique indicated the possibility to obtain a transparent ceramic of different types and in the future to improve the optical properties by eliminating pores. This suggests a potential method to increase the transparency of oxide ceramics with high melting temperatures.

Acknowledgements – Support from the 2016/23/D/ST8/00014 (National Science Centre, Poland) grants is gratefully acknowledged. The authors would like to thank Prof. Franciszek Krok for the possibility to use the SEM equipment. Part of the research was carried out with the equipment purchased with financial support from the European Regional Development Fund within the framework of the Polish Innovation Economy Operational Program (Contract No. POIG.02.01.00-12-023/08). The authors would also like to thank Dr. Teresa Jaworska-Gołąb for preliminary XRD measurements.

References

[1] LE ZHANG, ZHIGANG JIANG, QING YAO, ZHONGYING WANG, YIKUN ZHANG, SHUAI WEI, TIANYUAN ZHOU, YUE BEN, RONG SUN, HAO CHEN, *Stirring speed assisted homogenization of precipitation reaction for enhanced optical performance of Y_2O_3 transparent ceramics*, Ceramics International **44**(5), 2018, pp. 4967–4972, DOI: 10.1016/j.ceramint.2017.12.090.

[2] DENG S.Q., XUE Z.P., YANG Y.H., YANG Q., LIU Y.L., *Template-free fabrication and luminescent characterization of highly uniform and monodisperse $Y_2O_2S:Sm^{3+}$ hollow submicrospheres*, Journal of Materials Science and Technology **28**(7), 2012, pp. 666–672, DOI: 10.1016/S1005-0302(12)60114-5.

[3] WOOK KI JUNG, HO JIN MA, YOUNGTAE PARK, DO KYUNG KIM, *A robust approach for highly transparent Y_2O_3 ceramics by stabilizing oxygen defects*, Scripta Materialia **137**, 2017, pp. 1–4, DOI: 10.1016/j.scriptamat.2017.04.036.

[4] MUKHERJEE S.T., SUDARSAN V., SASTRY P.U., PATRA A.K., TYAGI A.K., *Annealing effects on the microstructure of combustion synthesized Eu^{3+} and Tb^{3+} doped Y_2O_3 nanoparticles*, Journal of Alloys and Compounds **519**, 2012, pp. 9–14, DOI: 10.1016/j.jallcom.2011.10.080.

[5] KRUK A., MRÓZEK M., DOMAGAŁA J., BRYLEWSKI T., GAWLIK W., *Synthesis and physicochemical properties of yttrium oxide doped with neodymium and lanthanum*, Journal of Electronic Materials **43**(9), 2014, pp. 3611–3617, DOI: 10.1007/s11664-014-3250-y.

[6] LEI ZHANG, WEI PAN, *Structural and thermo-mechanical properties of Nd: Y_2O_3 transparent ceramics*, Journal of the American Ceramic Society **98**(10), 2015, pp. 3326–3331, DOI: 10.1111/jace.13735.

[7] BILJAN T., GAJOVIĆ A., MEIĆ Z., MEŠTROVIĆ E., *Preparation, characterization and luminescence of nanocrystalline Y_2O_3:Ho*, Journal of Alloys and Compounds **431**(1–2), 2007, pp. 217–220, DOI: 10.1016/j.jallcom.2006.05.050.

[8] SHANSHAN LI, BINGLONG LIU, JIANG LI, XINGWEN ZHU, WENBIN LIU, YUBAI PAN, JINGKUN GUO, *Synthesis of yttria nano-powders by the precipitation method: the influence of ammonium hydrogen carbonate to metal ions molar ratio and ammonium sulfate addition*, Journal of Alloys and Compounds **678**, 2016, pp. 258–266, DOI: 10.1016/j.jallcom.2016.03.072.

[9] SERIVALSATIT K., KOKUOZ B., YAZGAN-KOKUOZ B., KENNEDY M., BALLATO J., *Synthesis, processing, and properties of submicrometer-grained highly transparent yttria ceramics*, Journal of the American Ceramic Society **93**(5), 2010, pp. 1320–1325, DOI: 10.1111/j.1551-2916.2010.03601.x.

[10] YIHUA HUANG, DONGLIANG JIANG, JINGXIAN ZHANG, QINGLING LIN, ZHENGREN HUANG, *Sintering of transparent yttria ceramics in oxygen atmosphere*, Journal of the American Ceramic Society **93**(10), 2010, pp. 2964–2967, DOI: 10.1111/j.1551-2916.2010.03940.x.

[11] MIE G., *Beiträge zur Optik trüber Medien, speziell kolloidaler Metallösungen*, Annalen der Physik **330**(3), 1908, pp. 377–445, DOI: 10.1002/andp.19083300302.

[12] HAJIZADEH-OGHAZ M., RAZAVI R.S., BAREKAT M., NADERI M., MALEKZADEH S., REZAZADEH M., *Synthesis and characterization of Y_2O_3 nanoparticles by sol-gel process for transparent ceramics applications*, Journal of Sol-Gel Science and Technology **78**(3), 2016, pp. 682–691, DOI: 10.1007/s10971-016-3986-3.

[13] XIANPENG QIN, GUOHONG ZHOU, HAO YANG, YAN YANG, JIAN ZHANG, SHIWEI WANG, *Synthesis and upconversion luminescence of monodispersed, submicron-sized Er^{3+}:Y_2O_3 spherical phosphors*, Journal of Alloys and Compounds **493**(1–2), 2010, pp. 672–677, DOI: 10.1016/j.jallcom.2009.12.188.

[14] ZHENG LI, LE ZHANG, TIANYUAN ZHOU, LIXI WANG, CHING PING WONG, HAO YANG, QITU ZHANG, *A novel spray co-precipitation method to prepare nanocrystalline Y_2O_3 powders for transparent ceramics*, Journal of Materials Science: Materials in Electronics **28**(6), 2017, pp. 4684–4689, DOI: 10.1007/s10854-016-6108-7.

[15] HUIQUN CAO, BING LU, HONG XIN, QI QIU, BIN YU, RUI MA, BIYU LIN, JINGJING CHEN, *Co-precipitation synthesis of YAG:Ce nanophosphor and vacuum sintering fabrication of transparent ceramics*, Science of Advanced Materials **9**(3–4), 2017, pp. 541–545.

[16] LIU B., LI J., YAVETSKIY R., IVANOV M., ZENG Y., XIE T., KOU H., ZHUO S., PAN Y., GUO J., *Fabrication of YAG transparent ceramics using carbonate precipitated yttria powder*, Journal of the European Ceramic Society **35**(8), 2015, pp. 2379–2390, DOI: 10.1016/j.jeurceramsoc.2015.02.014.

[17] TAXAK V.B., KHATKAR S.P., SANG-DO HAN, KUMAR R., KUMAR M., *Tartaric acid-assisted sol–gel synthesis of Y_2O_3:Eu^{3+} nanoparticles*, Journal of Alloys and Compounds **469**(1–2), 2009, pp. 224–228, DOI: 10.1016/j.jallcom.2008.01.088.

[18] ZHANG W., LU T.C., WEI N., SHI Y.L., MA B.Y., LUO H., ZHANG Z.B., DENG J., GUAN Z.G., ZHANG H.R., LI C.N., NIU R.H., *Co-precipitation synthesis and vacuum sintering of Nd:YAG powders for transparent ceramics*, Materials Research Bulletin **70**, 2015, pp. 365–372, DOI: 10.1016/j.materresbull.2015.04.063.

[19] KRUK A., BOBRUK M., ADAMCZYK A., MRÓZEK M., GAWLIK W., BRYLEWSKI T., *Preparation of yttria powders co-doped with Nd^{3+} and La^{3+} using EDTA gel processes for application in transparent ceramics*, Journal of the European Ceramic Society **37**(13), 2017, pp. 4129–4140, DOI: 10.1016/j.jeurceramsoc.2017.05.040.

[20] ATABAEV T.SH., HONG HA THI VU, HYUNG-KOOK KIM, YOON-HWAE HWANG, *The optical properties of Eu^{3+} and Tm^{3+} codoped Y_2O_3 submicron particles*, Journal of Alloys and Compounds **525**, 2012, pp. 8–13, DOI: 10.1016/j.jallcom.2012.01.148.

[21] NISSAMUDEEN K.M., GOPCHANDRAN K.G., *Y_2O_3:Eu^{3+} based nanophosphors with higher oscillator strength through lithium incorporation and indirect oxidation*, Journal of Alloys and Compounds **490**(1–2), 2010, pp. 399–406, DOI: 10.1016/j.jallcom.2009.10.018.

[22] KRUK A., WAJLER A., MROZEK M., ZYCH L., GAWLIK W., BRYLEWSKI T., *Transparent yttrium oxide ceramics as potential optical isolator materials*, Optica Applicata **45**(4), 2015, pp. 585–594, DOI: 10.5277/oa150413.

[23] LE ZHANG, ZHENG LI, FANGZHENG ZHEN, LIXI WANG, QITU ZHANG, RONG SUN, SELIM F.A., CHINGPING WONG, HAO CHEN, *High sinterability nano-Y_2O_3 powders prepared via decomposition of hydroxyl -carbonate precursors for transparent ceramics*, Journal of Materials Science **52**(14), 2017, pp. 8556 –8567, DOI: 10.1007/s10853-017-1071-0.

[24] LAKSHMINARASAPPA B.N., JAYARAMAIAH J.R., NAGABHUSHANA B.M., *Thermoluminescence of combustion synthesized yttrium oxide*, Powder Technology **217**, 2012, pp. 7–10, DOI: 10.1016/j.powtec.2011.09.042.

[25] LOJPUR V., MANCIC L., RABANAL M.E., DRAMICANIN M.D., TAN Z., HASHISHIN T., OHARA S., MILOSEVIC O., *Structural, morphological and luminescence properties of nanocrystalline up-converting $Y_{1.89}Yb_{0.1}Er_{0.01}O_3$ phosphor particles synthesized through aerosol route*, Journal of Alloys and Compounds **580**, 2013, pp. 584–591, DOI: 10.1016/j.jallcom.2013.07.125.

[26] ZHONGYING WANG, LE ZHANG, HAO YANG, JIAN ZHANG, LIXIWANG, QITU ZHANG, *High optical quality Y_2O_3 transparent ceramics with fine grain size fabricated by low temperature air pre-sintering and post-HIP treatment*, Ceramics International **42**(3), 2016, pp. 4238–4245, DOI: 10.1016/j.ceramint.2015.11.099.

[27] BINDU P., THOMAS S., *Estimation of lattice strain in ZnO nanoparticles: X-ray peak profile analysis*, Journal of Theoretical and Applied Physics **8**(4), 2014, pp. 123–134, DOI: 10.1007/s40094-014-0141-9.

[28] BAE J.S., SHIM K.S., KIM S.B., JEONG J.H., YI S.S., PARK J.C., *Photoluminescence characteristics of pulsed laser deposited $Y_{2-x}Gd_xO_3:Eu^{3+}$ thin film phosphors*, Journal of Crystal Growth **264**(1–3), 2004, pp. 290–296, DOI: 10.1016/j.jcrysgro.2003.12.075.

[29] TÄFFNER U., CARLE V., SCHÄFER U., HOFFMANN M.J., *Preparation and microstructural analysis of high -performance ceramics*, [In] *Metallography and Microstructures*, [Ed.] G.F. Vander Voort, Vol. 9, ASM Handbook, 2004, pp. 1057–1066, DOI: 10.31399/asm.hb.v09.a0003795.

[30] REPLIN Y., PROUST C., HUSSON E., BENY J.M., *Vibrational spectroscopy of the C-form of yttrium sesquioxide*, Journal of Solid State Chemistry **118**(1), 1995, pp. 163–169, DOI: 10.1006/jssc.1995.1326.

[31] PANDIT P., *Synthesis and characterization of Yb doped Y_2O_3 nanopowder for transparent laser host ceramic materials*, Materials Today: Proceedings **4**(2), 2017, pp. 3911–3917, DOI: 10.1016/j.matpr.2017.02.290.

[32] TAUC J., *Amorphous and Liquid Semiconductor*, Plenum, New York 1974.

[33] DIMITROV V., SAKKA S., *Electronic oxide polarizability and optical basicity of simple oxides*, Journal of Applied Physics **79**(3), 1996, pp. 1736–1740, DOI: 10.1063/1.360962.

[34] NIGARA Y., *Measurement of the optical constants of yttrium oxide*, Japanese Journal of Applied Physics **7**(4), 1968, pp. 404–408.

Received May 30, 2018
in revised form July 24, 2018